

AgentXRay: White-Boxing Agentic Systems via Workflow Reconstruction

Ruijie Shi¹, Houbin Zhang¹, Yuecheng Han², Yuheng Wang³, Jingru Fan², Runde Yang²

Yufan Dang¹, Huatao Li², Dewen Liu⁴, Yuan Cheng^{2†}, Chen Qian^{2†}

¹Tsinghua University, ²Shanghai Jiao Tong University, ³Wuhan University, ⁴Fudan University

srj22@mails.tsinghua.edu.cn, {qianc, cyuan328}@sjtu.edu.cn

Abstract

Large Language Models have shown strong capabilities in complex problem solving, yet many agentic systems remain difficult to interpret and control due to opaque internal workflows. While some frameworks offer explicit architectures for collaboration, many deployed agentic systems operate as black boxes to users. We address this by introducing Agentic Workflow Reconstruction (AWR), a new task aiming to synthesize an explicit, interpretable stand-in workflow that approximates a black-box system using only input–output access. We propose AgentXRay, a search-based framework that formulates AWR as a combinatorial optimization problem over discrete agent roles and tool invocations in a chain-structured workflow space. Unlike model distillation, AgentXRay produces editable white-box workflows that match target outputs under an observable, output-based proxy metric, without accessing model parameters. To navigate the vast search space, AgentXRay employs Monte Carlo Tree Search enhanced by a scoring-based Red-Black Pruning mechanism, which dynamically integrates proxy quality with search depth. Experiments across diverse domains demonstrate that AgentXRay achieves higher proxy similarity and reduces token consumption compared to unpruned search, enabling deeper workflow exploration under fixed iteration budgets.

1. Introduction

Large Language Models (LLMs) have exhibited remarkable capabilities in complex problem-solving, yet they continue to face bottlenecks stemming from their reliance on internalized parameters, which limits access to real-time information and specialized tools (Zhang et al., 2025; Lewis et al., 2020; Kandpal et al., 2023).

To transcend these limitations, standalone models have

[†]Corresponding authors.

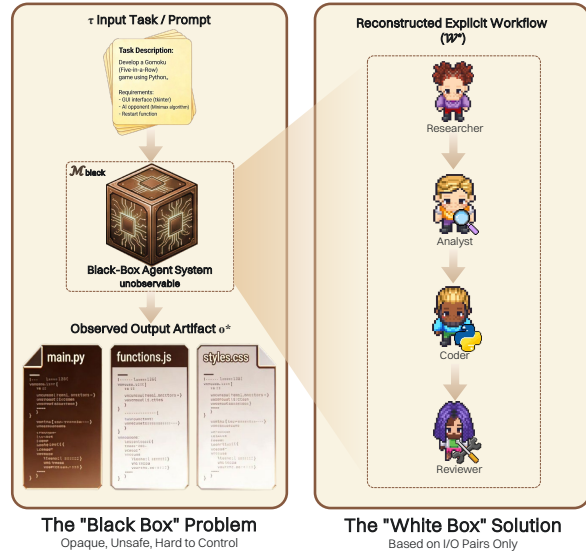


Figure 1. The concept of AWR. Given a black-box system $\mathcal{M}_{\text{black}}$ producing output o^* from input τ , the goal is to synthesize an explicit, interpretable white-box workflow \mathcal{W}^* (e.g., a sequence of specialized agents) that matches the target outputs under observable outputs, using only input-output pairs.

evolved into agents by incorporating dynamic planning, tool usage, and long-term memory (Xi et al., 2025; Liu et al., 2024b; Yao et al., 2023b; Schick et al., 2023; Wang et al., 2023a; Qin et al., 2023; Park et al., 2023; Shen et al., 2023) to expand their execution boundaries.

Along this line, Multi-Agent Systems (MAS) leverage collective intelligence through function specialization and structured collaboration (Li et al., 2023a; Wu et al., 2024), effectively addressing intricate tasks that demand multi-step reasoning and cross-domain expertise.

However, existing high-performance systems often operate as “black boxes”: their internal mechanisms—from sequential tool patterns to complex multi-agent topologies—remain opaque. The complexity of interactions further exacerbates this lack of interpretability (Domenech i Vila et al., 2024). Explaining agent behaviors is crucial for trustworthy AI, yet opacity remains a significant hurdle (Gimenez-Abalos

et al., 2024). Consequently, users struggle to comprehend decision-making processes, which limits adaptation to downstream tasks and hinders deployment in safety-critical domains (Salehi et al., 2025; Amodei et al., 2016; Bommasani, 2021; Hendrycks et al., 2021).

Motivated by this, we aim to build interpretable surrogate workflows (i.e., stand-in workflows) to improve transparency and controllability. We formally introduce **Agentic Workflow Reconstruction (AWR)**: given a dataset of Input-Output pairs collected from a black-box system, the goal is to synthesize an explicit white-box *surrogate* workflow (a stand-in workflow) that approximates the target behavior under an observable, output-based proxy metric.

We formulate AWR as a combinatorial optimization problem to identify the optimal configuration of agents and tools (Guo et al., 2024; Zhang et al., 2024b;a). Given the vast search space, we propose **AgentXRay**. We adopt the **linearity hypothesis** (Qian et al., 2025; Dang et al., 2025) to represent workflows as sequential trajectories, casting reconstruction as a search for high-scoring agentic primitives. To navigate this space, we employ **Monte Carlo Tree Search (MCTS)** (Yao et al., 2023a; Zhou et al., 2024), which effectively handles delayed rewards and balances exploration with exploitation. To mitigate the combinatorial explosion (Zhang et al., 2024a), we introduce a specialized **“Red-Black” Pruning mechanism**. This mechanism filters low-potential branches based on a multi-dimensional scoring function, concentrating resources on promising candidates. The resulting workflow serves as an interpretable proxy for the target system, enabling cost-effective adaptation.

We validate our framework across five domains: software development (ChatDev), data analysis (MetaGPT), education (TeachMaster), 3D modeling (ChatGPT), and scientific computing (Gemini). Empirical results demonstrate that AgentXRay recovers workflows with high *proxy* similarity (Static Functional Equivalence; avg. 0.426) and significantly improves search efficiency (8–22% token reduction) compared to unpruned baselines.

Our main contributions are:

- Task.** We introduce **AWR**, a new task that converts *black-box* LLM agent systems into *white-box* counterparts by reconstructing *explicit workflows* from input-output observations.
- Method.** We propose **AgentXRay**, an MCTS-based search framework equipped with a specialized **Red-Black Pruning** mechanism, which mitigates combinatorial explosion in the primitive space and enables practical reconstruction with improved search efficiency.
- Evaluation.** We validate AgentXRay across five do-

mains (*code generation, data analysis, education, scientific computing, 3D modeling*) by reconstructing representative systems (e.g., **ChatDev** (Qian et al., 2024), **MetaGPT** (Hong et al., 2023), **TeachMaster** (Wang et al., 2025), **ChatGPT** (GPT-5.2) and **Gemini 3 Pro**).

2. Method

2.1. Problem Formulation

We study *AWR*: constructing an interpretable surrogate workflow that matches a black-box system’s *final outputs* from input-output observations.

Task Definition and Inputs. Let $\mathcal{M}_{\text{black}} : \mathcal{X} \rightarrow \mathcal{Y}$ denote a black-box agentic system (including both multi-agent and complex single-agent workflows), where internal components (e.g., agent roles, prompts, and coordination topology) are hidden and only the I-O interface is accessible. We are given a dataset $\mathcal{D} = \{(\tau_i, o_i^*)\}_{i=1}^N$, where τ_i is a task description and $o_i^* = \mathcal{M}_{\text{black}}(\tau_i)$ is the corresponding output. Our goal is to synthesize a white-box workflow \mathcal{W} whose outputs match those of $\mathcal{M}_{\text{black}}$ under an evaluation metric.

Unified Primitive Space. We unify agents and tools into a single primitive space Ω of *agentic primitives*. Each primitive is a tuple $p = \langle \rho, \mu, \pi, T_{\text{local}} \rangle$, where ρ is the role, μ is the base model, π is the thought pattern, and T_{local} is the attached toolset. This definition treats both pure-reasoning agents ($T_{\text{local}} = \emptyset$) and tool-augmented agents ($T_{\text{local}} \neq \emptyset$) as atomic search units, consistent with tool-augmented LMs and API-based reasoning (Patil et al., 2024; Tang et al., 2023; Lu et al., 2023; Paranjape et al., 2023; Qin et al., 2023; Li et al., 2023b; Song et al., 2023).

Workflow Representation and Linearity. We represent a workflow \mathcal{W} as a linear sequence of length at most L_{\max} : $\mathbf{s} = [s_1, s_2, \dots, s_L]$ with $s_j \in \Omega$ and $1 \leq L \leq L_{\max}$. Searching arbitrary graph topologies is computationally prohibitive ($O(2^{|\Omega|^2})$). We therefore adopt the *Linearity Hypothesis* and restrict reconstruction to sequential workflows that capture the *execution-time ordering* of agent/tool calls.

This restriction is well-motivated by how many agentic systems are executed in practice. First, Qian et al. (2025) (MacNet) organizes multi-agent collaboration with DAG structures, but the system still executes agents in a *topological order*, which induces a concrete, time-ordered trace. Second, Dang et al. (2025) show that when an orchestrator is trained to dynamically coordinate agents without explicit topological constraints, effective coordination can still be realized as a compact chain-like policy under efficiency pressures. Moreover, many deployed LLM agents interact with their environment through an iterative *action–observation* loop, yielding a trajectory that is naturally linearizable; for example, ReAct interleaves reasoning with stepwise actions

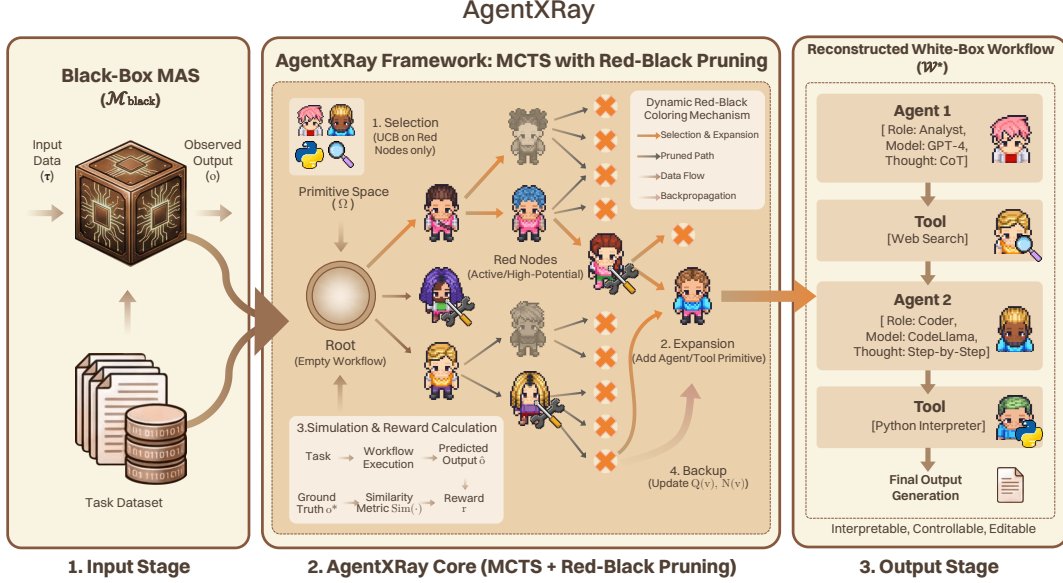


Figure 2. Overview of the AgentXRay framework. The process takes task inputs and black-box outputs, searches for a high-scoring primitive sequence via MCTS with Red-Black Pruning, and returns an interpretable white-box workflow.

conditioned on intermediate observations, and web agents evaluated in realistic environments such as WebArena operate as ordered sequences of atomic actions with feedback at each step (Yao et al., 2023c; Zhou et al., 2023).

These observations suggest that (i) complex coordination often *serializes* into an execution-time ordering even when the design is graph-structured, and (ii) sequential traces are the dominant observable object under strict black-box access. Our linearity hypothesis is therefore an execution-oriented surrogate that keeps reconstruction tractable while aligning with how agent systems behave at runtime.

Optimization Objective. We seek a workflow that maximizes the expected similarity between reconstructed outputs and black-box outputs on \mathcal{D} :

$$s^* = \arg \max_{s \in \Omega^{\leq L_{\max}}} \mathbb{E}_{(\tau, o^*) \sim \mathcal{D}} [\text{Sim}(\Phi(s, \tau), o^*)], \quad (1)$$

where $\Phi(s, \tau)$ denotes executing the workflow s on input τ , and $\text{Sim}(\cdot, \cdot) \in [0, 1]$ is a task-specific semantic/functional metric (implemented by an external evaluator; e.g., AST-based matching for code or cosine similarity for text).

Behavioral Fidelity as the Reconstruction Goal. Our objective is to reconstruct a workflow whose **input–output behavior** matches the target system: for the same input, the reconstructed system should produce an output as similar as possible to the target output, regardless of internal traces or implementation choices. In open-ended, multi-file settings, directly verifying true functional equivalence can be infea-

sible (non-portable environments, external tools/services, stochastic APIs, safety constraints). We therefore optimize *behavioral fidelity* using scalable **proxy** metrics (e.g., SFE) that approximate output-level consistency at scale.

2.2. AgentXRay

We propose *AgentXRay*, an MCTS-based search procedure over workflow prefixes.

MCTS States and Actions. Each tree node v represents a partial workflow prefix $s_{1:t}$ (the root is the empty prefix), and an edge corresponds to appending one primitive $p \in \Omega$. This view applies uniformly to multi-agent and single-agent settings: the search composes an explicit sequence of role/tool primitives to form s . We use MCTS (Kocsis & Szepesvári, 2006; Auer et al., 2002; Browne et al., 2012) to address delayed feedback: $\text{Sim}(\cdot)$ is only observable after executing (nearly) complete workflows. UCB (Auer et al., 2002) balances exploration and exploitation over a large heterogeneous action space. To control branching, AgentXRay maintains a *dynamic Red-Black coloring* that guides whether the search prioritizes depth refinement or width expansion.

2.2.1. SEARCH CYCLE

Each iteration performs selection/expansion, simulation, and backup:

1. Color-Guided Selection/Expansion. Let v be the current

node. If v is RED, we treat its current choice as stabilized and select among existing children using UCB to continue descending (depth refinement). If v is BLACK, we prioritize width exploration by creating a new child of v (branching), thus increasing the number of v 's children.

2. Simulation (Rollout). For a newly expanded node, we complete the workflow by sampling primitives until reaching length L_{\max} , execute the resulting workflow on a sampled task τ , and obtain output o . We use early stopping: if execution fails (e.g., primitive error or generation failure), we assign reward $r = 0$. Otherwise, $r = \text{Sim}(o, o^*)$.

3. Backup. We backpropagate r along the visited path, updating $N(v) \leftarrow N(v) + 1$ and $Q(v) \leftarrow Q(v) + r$ for all ancestors.

2.2.2. DYNAMIC RED-BLACK COLORING AND PRUNING

To identify robust structural backbones during noisy early exploration, we assign each node a composite potential score based on *Quality*, *Depth*, and *Width*:

$$\text{Score}(v) = \underbrace{\frac{Q(v)}{N(v)}}_{\text{Quality}} \cdot \underbrace{\left(\frac{d(v) + 1}{L_{\max} + 1} \right)}_{\text{Depth}} \cdot \underbrace{\frac{|\mathcal{C}(v)|}{M}}_{\text{Width}}, \quad (2)$$

where $d(v)$ is the depth (prefix length), $|\mathcal{C}(v)|$ is the number of children, and M is the maximum allowed number of children per node (a branching cap; in our implementation this corresponds to MAX_CHILDREN_NUMBER).

Let $\mathcal{L}_{\text{term}}$ denote the set of terminal nodes that should not be further expanded, including nodes that have reached depth L_{\max} and nodes marked terminal due to execution failures during rollout (early stopping). At each iteration, we compute the β -quantile θ_β of $\text{Score}(\cdot)$ over active nodes and assign colors:

$$C(v) = \begin{cases} \text{RED}, & \text{if } \text{Score}(v) \geq \theta_\beta \wedge v \notin \mathcal{L}_{\text{term}}, \\ \text{BLACK}, & \text{otherwise.} \end{cases} \quad (3)$$

2.3. Theoretical Complexity Analysis

We analyze how Red-Black Pruning contracts the search space and yields an exponential speedup in depth. This analysis characterizes search-space contraction under an effective (realized) pruning rate and serves as an explanatory bound; it does not claim regret-optimality guarantees for the full algorithm.

Let $b = |\Omega|$ be the branching factor, L_{\max} the maximum workflow length, and p the realized pruning rate induced by the scoring-and-threshold rule. Here p depends on the score distribution and the quantile parameter β , while β is a user-controlled threshold.

2.3.1. SEARCH SPACE CONTRACTION BOUNDS

Unpruned Baseline. Without pruning, the frontier size at depth d is $N_d = b^d$, and the total search volume is

$$\mathcal{V}_{\text{full}} = \sum_{d=0}^{L_{\max}} b^d = \frac{b^{L_{\max}+1} - 1}{b - 1} = \Theta(b^{L_{\max}}). \quad (4)$$

Lower Bound (Uniform Pruning). Under pruning rate p , the effective frontier is $\hat{N}_d = (b(1-p))^d$, yielding

$$\mathcal{V}_{\text{eff}} = \sum_{d=0}^{L_{\max}} (b(1-p))^d = \Theta((b(1-p))^{L_{\max}}). \quad (5)$$

Thus the acceleration ratio satisfies

$$\eta(L_{\max}) = \frac{\mathcal{V}_{\text{full}}}{\mathcal{V}_{\text{eff}}} \geq \left(\frac{1}{1-p} \right)^{L_{\max}}. \quad (6)$$

Upper Bound (β -Quantile Threshold). In an idealized aggressive case, the rule retains at most a $(1-\beta)$ fraction of nodes per depth, giving $\mathcal{V}_{\min} = \Theta((b(1-\beta))^{L_{\max}})$ and

$$\eta(L_{\max}) \leq \left(\frac{1}{1-\beta} \right)^{L_{\max}}. \quad (7)$$

These bounds characterize search-space contraction in an idealized asymptotic regime.

3. Experiments

We evaluate AgentXRay along three axes: (i) whether the unified primitive space can express diverse agentic behaviors, (ii) whether MCTS can recover high-fidelity workflows under strict black-box access, and (iii) whether Red-Black Pruning improves budget efficiency. We reconstruct workflows on five open-ended, tool-augmented domains covering both open-source multi-agent frameworks (ChatDev, MetaGPT, TeachMaster) and proprietary assistants (ChatGPT, Gemini).

3.1. Experimental Setup

Tasks and Benchmarks. We reconstruct five domains: (1) **Software Development**: ChatDev (Qian et al., 2024) on multi-file Python generation tasks from SRDD. (2) **Data Analysis**: MetaGPT (Hong et al., 2023) on MatPlotBench (Yang et al., 2024). (3) **Education**: TeachMaster (Wang et al., 2025) on automated teaching video generation. (4) **3D Modeling**: ChatGPT on ScanRefer (Chen et al., 2020). (5) **Scientific Computing**: Gemini on SciBench (Wang et al., 2023b). We treat all targets as strict black boxes and collect only input–output pairs.

Baselines. We compare AgentXRay with four categories of methods that test different hypotheses: (1) **SFT**: supervised fine-tuning on input–output pairs (Touvron et al., 2023), testing whether behavior cloning can capture agentic work-

Table 1. Reconstruction performance comparison across five domains. We report similarity scores where higher is better. **Bold** indicates the best result, and underlined indicates the second best. Subscript arrows indicate the performance gap compared to the strong baseline AFLOW (\uparrow improvement, \downarrow decline). \dagger denotes a statistically significant difference ($p \leq 0.05$) between a method and the strong baseline AFLOW.

| METHOD | CHATDEV | METAGPT | TEACHMASTER | 3D MODELING | SCI | AVG |
|-----------------------|---|---|---|---|---|----------------------------------|
| SFT | 0.355 \dagger _{0.048} | 0.272 \downarrow _{0.008} | 0.124 \dagger _{0.224} | 0.091 \dagger _{0.199} | 0.139 \dagger _{0.234} | 0.196 \dagger |
| CLAUDE | 0.256 \dagger _{0.147} | 0.322 \uparrow _{0.042} | 0.303 \dagger _{0.045} | 0.282 \downarrow _{0.008} | 0.299 \dagger _{0.074} | 0.292 \dagger |
| REACT | 0.267 \dagger _{0.136} | 0.331 \uparrow _{0.051} | 0.322 \downarrow _{0.026} | 0.270 \downarrow _{0.020} | 0.305 \dagger _{0.068} | 0.299 \dagger |
| AFLOW | 0.403 | 0.280 | 0.348 | 0.290 | 0.373 | 0.339 |
| AGENTXRAY w/o Tools | 0.413 \uparrow _{0.010} | 0.301 \dagger _{0.021} | 0.357 \dagger _{0.009} | 0.332 \dagger _{0.042} | 0.378 \dagger _{0.005} | 0.356 \dagger |
| AGENTXRAY w/o Pruning | 0.286 \dagger _{0.117} | 0.334 \uparrow _{0.054} | 0.378 \uparrow _{0.030} | 0.279 \downarrow _{0.011} | 0.312 \dagger _{0.061} | 0.318 |
| AGENTXRAY (Selected) | 0.509\dagger _{0.106} | <u>0.470\dagger</u> _{0.190} | 0.399\dagger _{0.051} | 0.318 \uparrow _{0.028} | 0.407\dagger _{0.034} | <u>0.421\dagger</u> |
| AGENTXRAY (All Tools) | 0.425 \dagger _{0.022} | 0.557\dagger _{0.277} | 0.390 \dagger _{0.042} | 0.362\dagger _{0.072} | 0.395 \dagger _{0.022} | 0.426\dagger |

flows; (2) **Claude Opus 4.5**: a strong single-model baseline with multi-turn self-refinement (Madaan et al., 2023), testing whether raw model capacity can substitute for structured search; (3) **ReAct (Claude Opus 4.5)**: Claude Opus 4.5 with ReAct-style tool use (Yao et al., 2023c), testing whether tool augmentation alone bridges the gap; (4) **AFlow**: MCTS-based workflow search without Red-Black Pruning (Zhang et al., 2024b), isolating our pruning contribution.

Notably, the Claude baselines use a stronger model than any component in AgentXRay’s primitive space. To reduce prompt sensitivity for the strong single-model baselines, we evaluate a small set of prompt variants and report the best-performing variant under the fixed interaction budget.

Budget Parity Protocol. We fix a max number of interaction rounds for every method, where one round equals one model invocation (including any internal self-refinement). All methods share the same tool set and per-round tool limits; token usage is measured and reported post hoc.

Implementation Details. We leverage both proprietary and open-weight LLMs to construct the primitive space, and access all models via API endpoints. Proprietary models include gpt-4-turbo, gpt-4, gpt-4o-mini, and gpt-3.5-turbo (Achiam et al., 2023). We additionally include strong third-party models served via compatible APIs, including claude-sonnet-4-20250514. Open-weight models include llama-4-maverick-17b-128e-instruct (Dubey et al., 2024), deepseek-v3.2 (Liu et al., 2024a), qwen3-coder-30b-a3b-instruct (Yang et al., 2025), and glm-4.7 (Zeng et al., 2022).

Evaluation Metric. We measure *proxy fidelity*: given the same input, does the reconstructed workflow produce an output artifact similar to the target system, regardless of unobservable internal traces. Because targets are strict black boxes and executing open-ended multi-file outputs can be costly or non-portable, we adopt **Static Functional Equiva-**

lence (SFE) (Ren et al., 2020) as a scalable proxy metric.

Human validation of SFE. To validate SFE as a proxy for *output-level* similarity, we conduct a small-scale blind human study with three annotators on 30 stratified-randomly sampled output pairs across domains and SFE score ranges. Human similarity scores (0–1) are positively correlated with SFE (Spearman $\rho=0.61$, $p<0.001$, 95% CI [0.30, 0.80]); inter-annotator agreement is moderate (Krippendorff’s $\alpha=0.57$).

3.2. Main Results

Table 1 reports the reconstruction performance across five domains. We organize our analysis around the hypotheses tested by each baseline category.

Overall Performance. AgentXRay achieves the best reconstruction fidelity across all five domains, with an average SFE of **0.426** (vs. Aflow 0.339 and Claude Opus 4.5 + ReAct 0.299) under the same interaction budget. Gains are consistent across heterogeneous targets, indicating that explicit workflow search over agentic primitives is a robust approach to AWR.

Can Behavior Cloning Suffice? SFT performs worst (avg. 0.196), especially on Education and 3D, suggesting that direct input→output cloning is inadequate for agentic systems. The key limitation is missing supervision on intermediate decomposition and tool-logic: input-output pairs do not reveal the underlying primitive sequence, so SFT may match surface form but fails to recover procedural structure (tool calls, control flow, coordination) (Pomerleau, 1991; Ross et al., 2011; De Haan et al., 2019; Nagarajan et al., 2020).

Can Model Capacity Compensate for Lack of Structure? Even a stronger single model (Claude Opus 4.5) reaches 0.292, and adding ReAct yields only 0.299 under the shared budget, indicating that capacity alone does not reliably discover compositional workflows. In contrast, AgentXRay’s

Table 2. Impact of Red-Black Pruning on achieved search depth. Red denotes the proportion of nodes marked for deep exploration; Len denotes the final workflow length. Without pruning, search stagnates at $L = 2$; with pruning, search reaches deeper workflows.

| METHOD | CHATDEV | | METAGPT | | TEACHMASTER | | 3D | | SCI | |
|-------------|---------|----------|---------|-----|-------------|----------|-----|----------|-----|----------|
| | RED | LEN | RED | LEN | RED | LEN | RED | LEN | RED | LEN |
| W/O PRUNING | 0 | 2 | 0 | 2 | 0 | 2 | 0 | 2 | 0 | 2 |
| W/O TOOLS | 55 | 6 | 55 | 2 | 55 | 4 | 65 | 9 | 45 | 6 |
| ALL TOOLS | 55 | 6 | 55 | 2 | 60 | 5 | 55 | 2 | 55 | 6 |
| SEL. TOOLS | 45 | 6 | 50 | 4 | 45 | 6 | 60 | 6 | 65 | 6 |

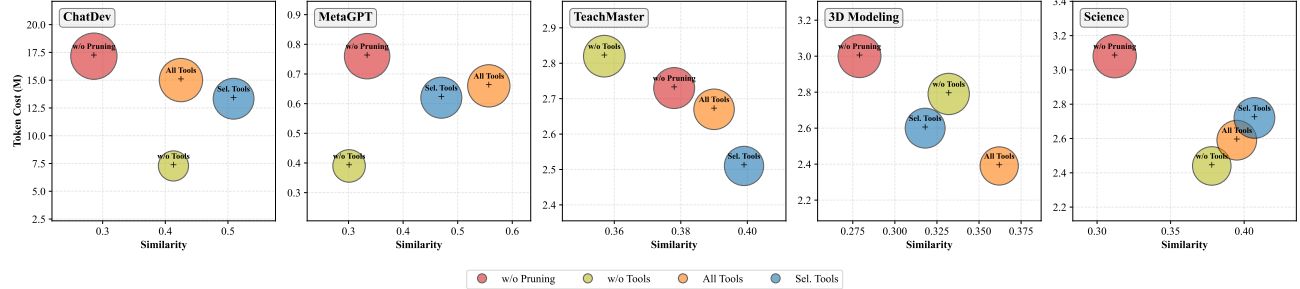


Figure 3. Cost-Efficiency analysis across five domains. The horizontal axis denotes reconstruction similarity (higher is better), while the vertical axis represents token consumption in millions (lower is better). Our method achieves comparable or higher fidelity than unpruned variants but with reduced computational overhead.

structured search explores and selects higher-fidelity workflow candidates within the same budget.

Does Pruning Matter? AgentXRay substantially outperforms AFlow (0.426 vs. 0.339 avg.), while removing pruning can even underperform AFlow (e.g., ChatDev: 0.286). This is because our unified primitive space increases the branching factor; without pruning, MCTS disperses the limited budget over many low-quality branches. Red-Black Pruning concentrates rollouts on high-potential prefixes, enabling deeper, coherent workflows under fixed N .

Cross-Domain Patterns. MetaGPT is most reconstructable (0.557), consistent with recurring analysis workflows well-covered by our primitive space, while ChatDev exhibits higher variance due to multi-file dependency sensitivity. Proprietary targets remain moderately reconstructable, supporting the feasibility of AWR under strict black-box access.

3.3. Ablation Study

We conduct systematic ablations to isolate the contribution of each component.

Tool Integration. Removing tools decreases average performance from 0.426 to 0.356 (-16.4%), with domain-dependent impact: substantial for MetaGPT (-46.0%) but marginal for Scientific Computing (-4.3%), reflecting whether the target system relies on external tool execution.

Pruning Enables Deeper Search. Table 2 shows that with-

out pruning, MCTS stagnates at shallow depth ($L = 2$) as the budget dissipates on the exponential frontier. With Red-Black Pruning, search reaches maximum depth ($L = 6$). The Red node proportions (45–65%) confirm that pruning concentrates budget on promising workflows, explaining AgentXRay’s superior performance.

3.4. Efficiency Analysis

Having validated reconstruction quality, we now turn to our third claim: Red-Black Pruning significantly improves search efficiency. This is critical for practical deployment, as the combinatorial search space would be intractable without effective pruning.

Token Consumption. Figure 3 illustrates the cost-efficiency trade-off across five domains. Comparing “AgentXRay (Sel. Tools)” with “AgentXRay w/o Pruning”, the Red-Black Pruning mechanism reduces token consumption by **8% to 22%** across all five domains, with the largest reduction on ChatDev (22.3%, from 17.16M to 13.33M tokens). The “w/o Tools” variant consumes the fewest tokens by avoiding tool execution overhead, but this comes at the cost of reconstruction quality (0.356 vs. 0.426 average, per Table 1). Our full method achieves a favorable balance: high reconstruction fidelity with substantially reduced cost.

The domain-specific patterns are also informative. ChatDev exhibits the highest consumption because multi-file code generation requires expensive repeated evaluation for each

workflow candidate. MetaGPT is the most efficient due to shorter interaction cycles and lighter verification. The remaining three domains cluster around 2.5–3.0M tokens, suggesting comparable evaluation overhead despite their diverse application areas.

Convergence Behavior. Figure 4 illustrates how reconstruction quality evolves with cumulative token consumption on two representative domains. Two key patterns emerge: (1) *Earlier convergence*—the pruned variants (“Sel. Tools” and “All Tools”) reach high-quality solutions within fewer tokens, while “w/o Pruning” requires substantially more budget to achieve comparable scores; (2) *Steeper ascent*—pruning concentrates exploration on promising branches, leading to faster quality improvement per token spent. For example, on ChatDev, “Sel. Tools” achieves 0.65+ score at \sim 10M tokens, whereas “w/o Pruning” requires \sim 12M tokens to reach the same level. These curves reflect training performance during MCTS; final test scores (Table 1) are evaluated separately.

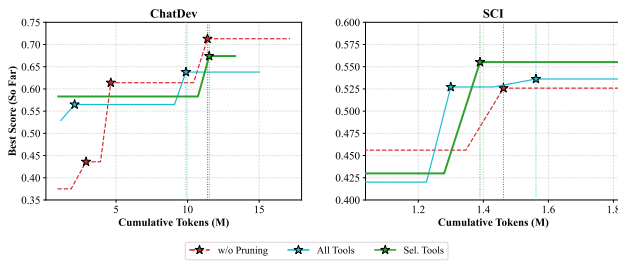


Figure 4. Convergence analysis on ChatDev and SCI. Pruned variants converge earlier and faster, reaching strong candidates at lower token cost than unpruned search.

Practical Considerations. Our complexity analysis characterizes search-space contraction in an idealized asymptotic regime; the empirical token savings (8–22%) are smaller but consistent with the qualitative prediction that pruning enables deeper, more focused exploration. Token consumption is measured uniformly for AgentXRay and all baselines under the same interaction budget, including strong single-model baselines with self-refinement.

Statistical Robustness. To assess reproducibility despite API-based non-determinism, we conducted 5-seed runs across representative domains and performed paired t-tests against AFlow. Results marked with † in Table 1 indicate statistically significant improvements ($p < 0.05$). Key findings: (1) All “AgentXRay” variants with pruning achieve significant improvements over AFlow on average. (2) The relative ranking of methods is preserved across all seeds. (3) Even worst-case runs exceed AFlow, confirming that improvements are not artifacts of favorable seed selection. These results demonstrate that our methodology is robust to the stochasticity inherent in LLM API calls.

3.5. Generalization to Open-Source Models

A natural question arises: *does AgentXRay depend on proprietary models?* We conduct an additional experiment targeting **Atoms**¹, a multi-agent platform evolved from MetaGPT. We use the Automatic Slide Generation dataset (Sefid et al., 2021) containing 80 presentation generation tasks, and construct the primitive space using *exclusively open-weight models*.

Table 3. Reconstruction on Atoms using open-weight models.

| METHOD | SIMILARITY |
|----------------------------|--------------|
| SFT | 0.275 |
| AFLOW | 0.321 |
| AGENTXRAY w/o TOOLS | 0.275 |
| AGENTXRAY (SELECTED TOOLS) | 0.326 |
| AGENTXRAY w/o PRUNING | 0.328 |
| AGENTXRAY (ALL TOOLS) | 0.337 |

AgentXRay (All Tools) achieves the best performance (0.337), outperforming AFlow by 5.0%. The ablation trends mirror earlier domains, suggesting that AgentXRay’s effectiveness stems from its algorithmic design rather than privileged access to proprietary models.

4. Discussion

We formally introduce AWR as a research task: constructing an editable, interpretable *surrogate workflow* from black-box input–output observations, with the goal of matching the target system’s *final outputs* rather than recovering hidden internals. Unlike *workflow generation* (e.g., AFlow) that optimizes from scratch, or *model distillation* that transfers behavior into parameters, AWR yields explicit workflows—offering a complementary path for understanding, debugging, and reusing high-performing systems when internal designs are unavailable.

While AgentXRay demonstrates the feasibility of AWR, several limitations and future directions remain.

Search Efficiency. Our empirical efficiency gains (8–22% token reduction) are smaller than asymptotic bounds because we operate under strict budgets ($N = 20$). The main value of Red-Black Pruning is *budget allocation*—concentrating evaluations on high-potential paths. Future work could incorporate **step-level reward models** (Xia et al., 2025; Lightman et al., 2023; Uesato et al., 2022) to enable denser feedback and earlier credit assignment, reducing reliance on expensive full rollouts.

Workflow Representation. We adopt a linear (chain-structured) workflow space. For a broad class of agentic

¹<https://atoms.dev>

systems, the execution on a given input can often be reasonably abstracted as an (approximately) linearized sequence of decisions and tool calls (e.g., as recorded by step-by-step traces), making the chain abstraction a pragmatic first-order model. However, this abstraction does not cover scenarios involving true concurrency or asynchronous coordination (e.g., parallel tool calls, event-driven updates, or branching that induces multiple simultaneously active threads), where execution cannot be faithfully linearized without losing key structure. Extending AWR to such settings is an important direction for future work, requiring richer representations (e.g., typed DAGs) and search procedures that balance structural expressivity with interpretability.

Evaluation and Scope. Our metric measures output-level structural/semantic similarity between reconstructed and target artifacts, and is intentionally agnostic to unobservable internal traces in strict black-box settings. We therefore use SFE as a scalable *proxy* for behavioral similarity on the observed I/O distribution, rather than a guarantee of execution-level correctness.

Our evaluation focuses on code-centric domains, enabling rigorous SFE analysis. Many agentic tasks naturally produce code (data pipelines, automation, API orchestration), making this scope relevant. Extending AWR to purely natural language domains (e.g., creative writing, open-ended dialogue) would require new evaluation approaches—combining embedding-based semantic similarity with human judgment or LLM-as-judge protocols (Zheng et al., 2023). More broadly, AWR faces intrinsic limits when targets rely on proprietary tools or hidden capabilities unavailable to the reconstruction space; establishing theoretical bounds on reconstructibility remains an open problem.

5. Related Work

LLM-based Agents and Search. Recent work has increasingly focused on LLM-based agents that perform reasoning, planning, and tool use (Wei et al., 2022; Yao et al., 2023a; Hao et al., 2023; Wang et al., 2023a; Schick et al., 2023; Qin et al., 2023). A common theme is to treat agent decision-making as search: Tree of Thoughts (ToT) (Yao et al., 2023a) generalizes Chain-of-Thought (CoT) into a tree, while RAP (Hao et al., 2023) and LATS (Zhou et al., 2024) integrate MCTS with LLMs to guide multi-step reasoning. These methods primarily focus on *instance-level* search for solving a single problem instance, whereas our work targets *workflow-level reconstruction*: identifying a generic, interpretable workflow structure that matches a black-box agent system across a dataset.

LLM-based Multi-Agent Systems and Automated Design. Multi-agent frameworks such as CAMEL (Li et al., 2023a), ChatDev (Qian et al., 2024), and MetaGPT (Hong

et al., 2023) coordinate multiple agents through natural language to divide roles and collaboratively solve complex tasks. Beyond manually designed systems, a growing body of work explores automated construction and optimization of multi-agent systems, including search-based methods like AFlow (Zhang et al., 2024b) and ADAS (Guo et al., 2024), as well as optimization-based methods like DyLAN (Liu et al., 2024b) and AgentPrune (Zhang et al., 2024a). In contrast, these approaches typically assume access to a configurable (white-box) agent architecture to optimize performance, whereas we study the complementary problem of reconstructing an explicit workflow from black-box input-output observations, applicable to both multi-agent and complex single-agent settings.

Interpreting Agentic Behaviors. Another related line aims to explain or interpret agent behaviors and decisions (Domenech i Vila et al., 2024; Gimenez-Abalos et al., 2024). These methods provide valuable insights into agent actions, but they do not explicitly reconstruct an executable, interpretable workflow structure of the underlying system, which is the goal of AWR.

6. Conclusion

We introduced AWR, a task that recovers an editable, interpretable white-box *surrogate* workflow for a black-box *agentic system* using only input–output observations. We proposed AgentXRay, which formulates reconstruction as a combinatorial search over a *Unified Primitive Space* and solves it with MCTS enhanced by *Red-Black Pruning*. Across five diverse domains spanning both multi-agent frameworks and proprietary assistants, AgentXRay achieves higher *proxy fidelity* (Static Functional Equivalence) than behavior cloning (SFT) and an unpruned MCTS baseline (AFlow), while reducing practical search cost under a fixed budget. We discuss limitations and future directions (e.g., graph-structured workflows and stronger evaluators); our results suggest that meaningful, editable workflow structure can be recovered from black-box behavior, providing a practical step toward more transparent, controllable, and debuggable agentic systems.

Impact Statement

This paper presents work whose goal is to advance the field of LLM by improving the interpretability of multi-agent systems. While such techniques may indirectly influence downstream applications of agent-based systems, we do not foresee significant negative societal or ethical risks arising directly from this work.

References

- Achiam, J., Adler, S., Agarwal, S., Ahmad, L., Akkaya, I., Aleman, F. L., Almeida, D., Altenschmidt, J., Altman, S., Anadkat, S., et al. Gpt-4 technical report. In *arXiv preprint arXiv:2303.08774*, 2023.
- Amodei, D., Olah, C., Steinhardt, J., Christiano, P., Schulman, J., and Mané, D. Concrete problems in ai safety. In *arXiv preprint arXiv:1606.06565*, 2016.
- Auer, P., Cesa-Bianchi, N., and Fischer, P. Finite-time analysis of the multiarmed bandit problem. In *Machine learning*, 2002.
- Bommasani, R. On the opportunities and risks of foundation models. In *arXiv preprint arXiv:2108.07258*, 2021.
- Browne, C. B., Powley, E., Whitehouse, D., Lucas, S. M., Cowling, P. I., Rohlfsen, P., Tavener, S., Perez, D., Samothrakis, S., and Colton, S. A survey of monte carlo tree search methods. In *IEEE Transactions on Computational Intelligence and AI in games*, 2012.
- Chen, D. Z., Chang, A. X., and Nießner, M. Scanrefer: 3d object localization in rgb-d scans using natural language. In *European Conference on Computer Vision (ECCV)*, 2020.
- Dang, J., Qian, C., et al. Multi-agent collaboration via evolving orchestration. In *arXiv preprint arXiv:2505.19591*, 2025.
- De Haan, P., Jayaraman, D., and Levine, S. Causal confusion in imitation learning. In *Advances in Neural Information Processing Systems (NeurIPS)*, 2019.
- Domenech i Vila, M., Gnatyshak, D., Tormos, A., Gimenez-Abalos, V., and Alvarez-Napagao, S. Explaining the behaviour of reinforcement learning agents in a multi-agent cooperative environment using policy graphs. In *Electronics*, 2024.
- Dubey, A., Jauhri, A., Pandey, A., Kadian, A., Al-Dahle, A., Letman, A., Mathur, A., Schelten, A., Yang, A., Fan, A., et al. The llama 3 herd of models. In *arXiv e-prints*, 2024.
- Gimenez-Abalos, V., Alvarez-Napagao, S., Tormos, A., Cortés, U., and Vázquez-Salceda, J. Intention-aware policy graphs: answering what, how, and why in opaque agents. In *arXiv preprint arXiv:2409.19038*, 2024.
- Guo, S., Ren, X., et al. Automated design of agentic systems. In *arXiv preprint arXiv:2408.08435*, 2024.
- Hao, S., Gu, Y., Ma, H., Hong, J., Wang, Z., Wang, D., and Hu, Z. Reasoning with language model is planning with world model. In *Proceedings of the 2023 Conference on Empirical Methods in Natural Language Processing (EMNLP)*, 2023.
- Hendrycks, D., Carlini, N., Schulman, J., and Steinhardt, J. Unsolved problems in ml safety. In *arXiv preprint arXiv:2109.13916*, 2021.
- Hong, S., Zhuge, M., Chen, J., Zheng, X., Cheng, Y., Wang, J., Zhang, C., Wang, Z., Yau, S. K. S., Lin, Z., et al. Metagpt: Meta programming for a multi-agent collaborative framework. In *International Conference on Learning Representations (ICLR)*, 2023.
- Kandpal, N., Deng, H., Roberts, A., Wallace, E., and Raffel, C. Large language models struggle to learn long-tail knowledge. In *International Conference on Machine Learning (ICML)*, 2023.
- Kocsis, L. and Szepesvári, C. Bandit based monte-carlo planning. In *European conference on machine learning*, 2006.
- Lewis, P., Perez, E., Piktus, A., Petroni, F., Karpukhin, V., Goyal, N., Küttler, H., Lewis, M., Yih, W.-t., Rocktaschel, T., et al. Retrieval-augmented generation for knowledge-intensive nlp tasks. In *Advances in neural information processing systems*, 2020.
- Li, G., Hammoud, H. A. A. K., Itani, H., Khizbullin, D., and Ghanem, B. Camel: Communicative agents for "mind" exploration of large language model society. In *Advances in Neural Information Processing Systems (NeurIPS)*, 2023a.
- Li, M., Zhao, Y., Yu, B., Song, F., Li, H., Yu, H., Li, Z., Huang, F., and Li, Y. Api-bank: A comprehensive benchmark for tool-augmented llms. In *arXiv preprint arXiv:2304.08244*, 2023b.
- Lightman, H., Kosaraju, V., Burda, Y., Edwards, H., Baker, B., Lee, T., Leike, J., Schulman, J., Sutskever, I., and Cobbe, K. Let's verify step by step. In *The Twelfth International Conference on Learning Representations (ICLR)*, 2023.
- Liu, A., Feng, B., Xue, B., Wang, B., Wu, B., Lu, C., Zhao, C., Deng, C., Zhang, C., Ruan, C., et al. Deepseek-v3 technical report. In *arXiv preprint arXiv:2412.19437*, 2024a.
- Liu, Z., Hu, H., Zhang, S., Guo, H., Zhang, K., Liu, Z., and Zhao, Z. Dynamic llm-agent network: An llm-agent collaboration framework with qualitative and quantitative evaluation. In *Association for Computational Linguistics (ACL)*, 2024b.

- Lu, P., Peng, B., Cheng, H., Galley, M., Chang, K.-W., Wu, Y. N., Zhu, S.-C., and Gao, J. Chameleon: Plug-and-play compositional reasoning with large language models. In *Advances in Neural Information Processing Systems (NeurIPS)*, 2023.
- Madaan, A., Tandon, N., Gupta, P., Hallinan, S., Gao, L., Wiegreffe, S., Alon, U., Dziri, N., Prabhumoye, S., Yang, Y., et al. Self-refine: Iterative refinement with self-feedback. In *Advances in Neural Information Processing Systems (NeurIPS)*, 2023.
- Nagarajan, V., Andreassen, A., and Neyshabur, B. Understanding the failure modes of out-of-distribution generalization. In *arXiv preprint arXiv:2010.15775*, 2020.
- Paranjape, B., Lundberg, S., Singh, S., Hajishirzi, H., Zettlemoyer, L., and Ribeiro, M. T. Art: Automatic multi-step reasoning and tool-use for large language models. In *arXiv preprint arXiv:2303.09014*, 2023.
- Park, J. S., O'Brien, J., Cai, C. J., Morris, M. R., Liang, P., and Bernstein, M. S. Generative agents: Interactive simulacra of human behavior. In *ACM Symposium on User Interface Software and Technology (UIST)*, 2023.
- Patil, S. G., Zhang, T., Wang, X., and Gonzalez, J. E. Gorilla: Large language model connected with massive apis. In *Advances in Neural Information Processing Systems (NeurIPS)*, 2024.
- Pomerleau, D. A. Efficient training of artificial neural networks for autonomous navigation. In *Neural computation*, 1991.
- Qian, C., Liu, W., Liu, H., Chen, N., Dang, Y., Li, J., Yang, C., Chen, W., Su, Y., Cong, X., et al. Chatdev: Communicative agents for software development. In *Proceedings of the 62nd Annual Meeting of the Association for Computational Linguistics (ACL)*, 2024.
- Qian, C., Xie, Z., Wang, Y., Liu, W., Zhu, K., Xia, H., Dang, Y., Du, Z., Chen, W., Yang, C., et al. Scaling large language model-based multi-agent collaboration. In *International Conference on Learning Representations (ICLR)*, 2025.
- Qin, Y., Liang, S., Ye, Y., Zhu, K., Yan, L., Lu, Y., Lin, Y., Cong, X., Tang, X., Qian, B., et al. Toolllm: Facilitating large language models to master 16000+ real-world apis. In *International Conference on Learning Representations (ICLR)*, 2023.
- Ren, S., Guo, D., Lu, S., Zhou, L., Liu, S., Tang, D., Sundaresan, N., Zhou, M., Blanco, A., and Ma, S. Codebleu: A method for automatic evaluation of code synthesis. In *arXiv preprint arXiv:2009.10297*, 2020.
- Ross, S., Gordon, G., and Bagnell, D. A reduction of imitation learning and structured prediction to no-regret online learning. In *Proceedings of the fourteenth international conference on artificial intelligence and statistics*, 2011.
- Salehi, S., Singh, Y., Habibi, P., and Erickson, B. J. Beyond single systems: How multi-agent ai is reshaping ethics in radiology. In *Bioengineering*, 2025.
- Schick, T., Dwivedi-Yu, J., Dessì, R., Raileanu, R., Lomeli, M., Hambro, E., Zettlemoyer, L., Cancedda, N., and Scialom, T. Toolformer: Language models can teach themselves to use tools. In *Advances in Neural Information Processing Systems (NeurIPS)*, 2023.
- Sefid, A., Mitra, P., Wu, J., and Giles, C. L. Extractive research slide generation using windowed labeling ranking. In *Proceedings of the Second Workshop on Scholarly Document Processing*, 2021.
- Shen, Y., Song, K., Tan, X., Li, D., Lu, W., and Zhuang, Y. Hugginggpt: Solving ai tasks with chatgpt and its friends in hugging face. In *Advances in Neural Information Processing Systems (NeurIPS)*, 2023.
- Song, Y., Xiong, W., Zhu, D., Wu, W., Qian, H., Song, M., Huang, H., Li, C., Wang, K., Yao, R., et al. Restgpt: Connecting large language models with real-world restful apis. In *arXiv preprint arXiv:2306.06624*, 2023.
- Tang, Q., Deng, Z., Lin, H., Han, X., Liang, Q., Cao, B., and Sun, L. Toolalpaca: Generalized tool learning for language models with 3000 simulated cases. In *arXiv preprint arXiv:2306.05301*, 2023.
- Touvron, H., Martin, L., Stone, K., et al. Llama 2: Open foundation and fine-tuned chat models. In *arXiv preprint arXiv:2307.09288*, 2023.
- Uesato, J., Kushman, N., Kumar, R., Song, F., Siegel, N., Wang, L., Creswell, A., Irving, G., and Higgins, I. Solving math word problems with process-and outcome-based feedback. In *arXiv preprint arXiv:2211.14275*, 2022.
- Wang, G., Xie, Y., Jiang, Y., Mandlekar, A., Xiao, C., Zhu, Y., Fan, L., and Anandkumar, A. Voyager: An open-ended embodied agent with large language models. In *arXiv preprint arXiv:2305.16291*, 2023a.
- Wang, X., Hu, Z., Lu, P., Zhu, Y., Zhang, J., Subramaniam, S., Loomba, A. R., Zhang, S., Sun, Y., and Wang, W. Scibench: Evaluating college-level scientific problem-solving abilities of large language models. In *arXiv preprint arXiv:2307.10635*, 2023b.
- Wang, Y., Yang, R., Wu, L., Zhang, J., Fan, J., Fu, R., Zhou, T., Li, H., Chen, S., E, W., and Qian, C. Generative teaching via code. In *arXiv preprint arXiv:2601.04204*, 2025.

- Wei, J., Wang, X., Schuurmans, D., Bosma, M., Chi, E., Le, Q., and Zhou, D. Chain-of-thought prompting elicits reasoning in large language models. In *Advances in Neural Information Processing Systems (NeurIPS)*, 2022.
- Wu, Q., Bansal, G., Zhang, J., Wu, Y., Li, B., Zhu, E., Jiang, L., Zhang, X., Zhang, S., Liu, J., et al. Autogen: Enabling next-gen llm applications via multi-agent conversations. In *First Conference on Language Modeling (COLM)*, 2024.
- Xi, Z., Chen, W., Guo, X., He, W., Ding, Y., Hong, B., Zhang, M., Wang, J., Jin, S., Zhou, E., et al. The rise and potential of large language model based agents: A survey. In *Science China Information Sciences*, 2025.
- Xia, Y., Fan, J., Chen, W., Yan, S., Cong, X., Zhang, Z., Lu, Y., Lin, Y., Liu, Z., and Sun, M. Agentrm: Enhancing agent generalization with reward modeling. In *arXiv preprint arXiv:2502.18407*, 2025.
- Yang, A., Li, A., Yang, B., Zhang, B., Hui, B., Zheng, B., Yu, B., Gao, C., Huang, C., Lv, C., et al. Qwen3 technical report. In *arXiv preprint arXiv:2505.09388*, 2025.
- Yang, Z., Zhou, Z., Wang, S., Cong, X., Han, X., Yan, Y., Liu, Z., Tan, Z., Liu, P., Yu, D., Liu, Z., Shi, X., and Sun, M. Matplotagent: Method and evaluation for llm-based agentic scientific data visualization. In *arXiv preprint arXiv:2402.11453*, 2024.
- Yao, S., Yu, D., Zhao, J., Shafran, I., Griffiths, T. L., Cao, Y., and Narasimhan, K. Tree of thoughts: Deliberate problem solving with large language models. In *arXiv preprint arXiv:2305.10601*, 2023a.
- Yao, S., Zhao, J., Yu, D., Du, N., Shafran, I., Narasimhan, K., and Cao, Y. React: Synergizing reasoning and acting in language models. In *International Conference on Learning Representations (ICLR)*, 2023b.
- Yao, S., Zhao, J., Yu, D., Du, N., Shafran, I., Narasimhan, K., and Cao, Y. React: Synergizing reasoning and acting in language models. In *International Conference on Learning Representations (ICLR)*, 2023c.
- Zeng, A., Liu, X., Du, Z., Wang, Z., Lai, H., Ding, M., Yang, Z., Xu, Y., Zheng, W., Xia, X., et al. Glm-130b: An open bilingual pre-trained model. In *arXiv preprint arXiv:2210.02414*, 2022.
- Zhang, G., Yue, Y., Li, Z., Yun, S., Wan, G., Wang, K., Cheng, D., Yu, J. X., and Chen, T. Cut the crap: An economical communication pipeline for llm-based multi-agent systems. In *The Thirteenth International Conference on Learning Representations (ICLR)*, 2024a.
- Zhang, J., Zhang, C., and Kamarthi, S. Aflow: Automating agentic workflow generation. In *arXiv preprint arXiv:2410.10762*, 2024b.
- Zhang, Y., Li, Y., Cui, L., Cai, D., Liu, L., Fu, T., Huang, X., Zhao, E., Zhang, Y., Chen, Y., et al. Siren’s song in the ai ocean: A survey on hallucination in large language models. In *Association for Computational Linguistics (ACL)*, 2025.
- Zheng, L., Chiang, W.-L., Sheng, Y., Zhuang, S., Wu, Z., Zhuang, Y., Lin, Z., Li, Z., Li, D., Xing, E. P., et al. Judging llm-as-a-judge with mt-bench and chatbot arena. In *Advances in Neural Information Processing Systems (NeurIPS)*, 2023.
- Zhou, A., Yan, K., Shlapentokh-Rothman, M., Wang, H., and Wang, Y.-X. Language agent tree search unifies reasoning, acting, and planning in language models. In *International Conference on Machine Learning (ICML)*, 2024.
- Zhou, S., Xu, F. F., Zhu, H., Zhou, X., Lo, R., Sridhar, A., Cheng, X., Ou, T., Bisk, Y., Fried, D., et al. Webarena: A realistic web environment for building autonomous agents. In *arXiv preprint arXiv:2307.13854*, 2023.